Quaternary Science Reviews 246 (2020) 106492

Contents lists available at ScienceDirect

Quaternary Science Reviews

journal homepage: www.elsevier.com/locate/quascirev

Present day Jakobshavn Isbræ close to the Holocene minimum extent

Karita Kajanto [a, *], Helene Seroussi [b], Basile de Fleurian [a], Kerim H. Nisancioglu [a, c]

[a] Department of Earth Science, University of Bergen and Bjerknes Centre for Climate Research, Bergen, Norway
[b] Jet Propulsion Laboratory, California Institute of Technology, Pasadena, CA, USA
[c] Centre for Earth Evolution and Dynamics, University of Oslo, Oslo, Norway

ARTICLE INFO

Article history:
Received 19 December 2019
Received in revised form
29 June 2020
Accepted 17 July 2020
Available online xxx

Keywords:
Jakobhsavn Isbræ
Holocene
Glaciology
Greenland
Marine terminating glaciers
Paleo ice-sheets
Modeling
Ice-ocean interaction

ABSTRACT

Marine terminating glaciers evolve on millenial timescales in response to changes in oceanic and atmospheric conditions. However, the relative role of oceanic and atmospheric drivers remains uncertain. The evolution of marine terminating glaciers under the warmer than present Holocene Climate Optimum climate can give important insights into the dynamics of ice streams as the climate evolves. The early Holocene evolution of Jakobshavn Isbræ, from the Last Glacial Maximum extent up to 8.2 ka BP is well constrained by geomorphological studies in the area. However, the Holocene minimum extent of the glacier is unknown. Here, we use a high-resolution regional ice sheet model to study the retreat and readvance of Jakobshavn Isbræ from the Mid-Holocene to the Little Ice Age. This model of Jakobshavn Isbræ accurately tracks the terrestrial ice margin and agrees with available estimates of marine grounding line evolution. We find that the Holocene minimum extent of both the terrestrial ice margin and the grounding line, reached at 6–5 ka BP, is close to the present day extent of the glacier. We also find that the glacier is currently located close to a tipping point, from beyond which readvance would require a longer and more significant cooling than the Little Ice Age. We assess the importance of the ocean forcing in explaining the Holocene evolution of Jakobshavn, and find that cooling within the fjord during the Mid-Holocene is critical for the glacier to readvance. This finding emphasizes the role of ocean forcing when trying to understand the millenial scale evolution of marine terminating glaciers.

1. Introduction

Marine terminating outlet glaciers are the main route of ice discharge in contemporary ice sheets and are sensitive to changes in external forcing (Schoof, 2007; Vieli and Nick, 2011; Nick et al., 2013; Enderlin et al., 2014; Aschwanden et al., 2016; Morlighem et al., 2016; Bondzio et al., 2017). Unfortunately, the physical processes controlling the behaviour of marine terminating glaciers are not implemented in large scale models used to study the long term evolution of ice sheets, such as Greenland, (e.g. Tarasov and Peltier, 2002; Fleming and Lambeck, 2004; Simpson et al., 2009; Lecavalier et al., 2014; Tabone et al., 2019; Cuzzone et al., 2019). There is also a large discrepancy between models of the deglaciation of the Greenland Ice Sheet (GIS) and the geomorphological evidence of the ice margin retreat in the vicinity of marine ice streams since the last glacial maximum (Lecavalier et al., 2014; Nielsen et al., 2018; Cuzzone et al., 2019). In order to correctly explain the recorded ice front evolution, the dynamics of marine terminating ice streams must be accurately incorporated in models. In large scale models, dynamical processes are often neglected due to coarse resolution and incomplete description of physical processes, both limited by computational power. For smaller catchments, however, dynamical modelling is tractable over millenial time scales.

Jakobshavn Isbræ (JI) is the fastest flowing ice stream in Greenland (Rignot and Mouginot, 2012), and also the largest contributor to dynamic discharge of the GIS in recent years (Enderlin et al., 2014). It has been studied extensively due to its high flow rate and dramatic thinning, acceleration, and retreat in the 2000's (Weidick and Bennike, 2007; Joughin et al., 2008; Csatho et al., 2008; Briner et al., 2010; Van Der Veen et al., 2011; Joughin et al., 2012; Nick et al., 2013; Young and Briner, 2015). JI has been modelled in several studies, but none of the regional models of the JI catchment extend prior to the Little Ice Age (LIA) maximum (Muresan et al., 2016; Bondzio et al., 2017; Steiger et al., 2018). The bed geometry of JI is distinctive and important in controlling the dynamics of the glacier. The mouth of Jakobshavn fjord has a

* Corresponding author. Department of Earth Science, University of Bergen and Bjerknes Centre for Climate Research, Jahnebakken 5, 5007, Bergen, Norway.
E-mail address: karita.kajanto@uib.no (K. Kajanto).

https://doi.org/10.1016/j.quascirev.2020.106492

shallow sill that is 255 m below the present-day sea level at the deepest point (Fig. 1a). Upstream of the sill, the fjord deepens quickly to at least 500 m, although the exact depth is unknown. Approximately 60 km inland from the sill, where the present day glacier terminus is located, the fjord bed has a small elevated bump. Upstream of the bump, the fjord deepens further and is characterised by a deep and narrow trough that continues over 100 km inland. A large portion of the JI catchment is below sea level (An et al., 2017; Morlighem et al., 2017).

Recent observations of water temperature and terminus position of JI indicate sensitivity of the glacier to ocean temperature, and that ocean-induced melt plays a signifcant role in controlling the glacier evolution even in the absence of a floating ice tongue (Khazendar et al., 2019). Lloyd et al. (2011) find that over the last century, the inflow of warm ocean water correlates with the retreat episodes of JI. This significance of ocean forcing to JI is also shown by modelling studies: Vieli and Nick (2011), Nick et al. (2013), Muresan et al. (2016), Bondzio et al. (2017), and Steiger et al. (2018) all found that the dynamic changes of JI in recent decades are largely driven by the ocean parameterization, and controlled by the fjord geometry. Thus, there is evidence that ocean forcing is crucial to a system such as JI, but the relative importance of the ocean forcing is poorly understood on longer than centennial time scales.

Despite the accumulated evidence that ocean forcing is important for marine terminating glaciers (e.g. Straneo et al., 2013), most Greenland deglaciation models have excluded fast-flowing ice streams and ocean forcing and focused on relative sea level and atmospheric forcing, often due to practical issues such as model resolution and computational time (Tarasov and Peltier, 2002; Simpson et al., 2009; Lecavalier et al., 2014). Tabone et al. (2019), studied the effect of millenial scale ocean variability on the GIS over the last glacial cycle, showing that the GIS is sensitive to changes in the ocean throughout the glaciation, even though the coarse resolution of the model prevents the inclusion of fast flowing ice streams. Thus, there is a need to study fast-flowing marine terminating ice streams on millenial timescales with sufficient model resolution.

Even though JI and the surrounding area have been extensively studied, and the evolution of the glacier starting from the LIA has been modelled in several studies, the Holocene retreat, the Holocene minimum extent, and the drivers controlling this retreat are not yet completely understood. Here, we use a high-resolution regional ice sheet model to study the retreat and readvance of JI from the Mid-Holocene to the LIA. We constrain the Holocene minimum extent of the glacier for both the terrestrial ice margin and the grounding line below sea level. To our knowledge this is the first regional model of JI that can track the grounding line over millenial timescales. In addition, we assess the importance of the ocean forcing in explaining the Holocene evolution of JI.

2. Deglaciation history of the Disko Bay region

This section summarizes published records of the Holocene evolution of JI and the Disko Bay region. We discuss the timing of events relevant for our study. For an account of the uncertainties related to these ages, we refer to the original papers.

2.1. Early Holocene retreat of the ice margin

The main features of the deglaciation of the Disko Bay area are summarized in Fig. 1. The large scale evolution of the ice margin is driven by the atmospheric forcing (Fig. 1b). During the Last Glacial Maximum (LGM) the Greenland Ice Sheet extended all the way to the continental shelf edge (O Cofaigh et al., 2013; Hogan et al., 2016). Deglaciation from the LGM extent of the paleo-predecessor of JI was underway by 14.9 ka BP, and the retreat was interrupted by a short readvance during the Younger Dryas period around 12.2 ka BP (O Cofaigh et al., 2013). After the Younger Dryas cooling, the ice margin retreated rapidly, reaching the western side of Disko Bay at approximately 11 ka BP, and the present day shoreline by 10 ka BP (Lloyd et al., 2005; O Cofaigh et al., 2013; Young and Briner, 2015; Streuff et al., 2017). The retreat rate decreased as the ice retreated eastwards, from hundreds of meters per year in Egedesminde Dyp down to tens of meters per year on the eastern side of Disko Bay, as shown in Fig. 1A (Streuff et al., 2017). Streuff et al. (2017) also present geomorphological and lithological evidence suggesting that the ice margin might have been grounded during the retreat, and a floating tongue only existed locally. Between 10 and 8 ka BP the ice edge retreated and stabilized on present day land areas, forming the terrestrial ice margin of the JI catchment (Young and Briner, 2015) (red lines in Fig. 1a).

During this period of relative stability, the marine part of JI remained grounded below sea level on the sill at the mouth of Jakobshavn's fjord, providing extensive sedimentation to Disko Bay (Lloyd et al., 2005; Hogan et al., 2012; Streuff et al., 2017). This period of standstill coincides with the Holocene thermal maximum around 10–8 ka BP (Fig. 1b) (Vinther et al., 2009), and it is plausible that despite the terrestrial ice margin being stable, the ice sheet was still experiencing thinning during this time. The terrestrial ice margin retreat in south-western Greenland, south of Disko Bay, did not experience a similar millenial-scale standstill period in the Mid-Holocene, but retreated continuously eastwards, reaching the LIA extent approximately at 6 ka BP (Lesnek and Briner, 2018).

2.2. Mid-Holocene retreat of JI and the Neoglacial readvance

The evolution of both the grounding line of JI and the terrestrial ice margin are poorly known between 8 ka BP and the LIA. Some time after 8 ka BP, JI ungrouded from the sill, and retreated into the fjord (Lloyd et al., 2005; Young and Briner, 2015; Streuff et al., 2017). Estimates on the exact timing of the retreat vary between 8.2 and 7.1 ka BP (black stars in Fig. 1a, (Lloyd et al., 2005; Streuff et al., 2017)). There is no evidence of the grounding line retreat rate within the fjord, but the deep retrograde topography indicates the possibility of rapid retreat induced by marine ice sheet instability (Schoof, 2007; Durand et al., 2009; Gudmundsson et al., 2012; Jamieson et al., 2012). Evidence of the retreat of the terrestrial ice margin surrounding the fjord suggests that the retreat was indeed rapid, and that the terrestrial ice margin had retreated inland of the LIA extent by 7 ka BP (Young and Briner, 2015). The Holocene minimum extent of the terrestrial ice margin is poorly constrained, and estimates vary between 15 and 100 km inland from the LIA position; the largest retreats are based on ice-sheet wide models, and the smaller retreats are based on evidence, such as moraines, lake sediments, and archaeological findings (Weidick et al., 1990; Tarasov and Peltier, 2002; Briner et al., 2010; Funder et al., 2011; Nielsen et al., 2018). However, there is no direct geomorphological evidence on the minimum extent of the grounding line in the fjord, nor is the retreat of the grounding line resolved well in models. Thus, there is no direct information on the position of the grounding line during the Mid-Holocene. Also, there is no direct evidence indicating if a floating tongue existed at some point during the retreat.

Estimates of the timing of the Neoglacial readvance of JI are also variable. Relative sea level data indicate that landscape submergence was already initiated by around 3 ka BP (Long et al., 2006), suggesting glacial advance, while radiocarbon ages of marine fauna in the LIA moraine give a minimum constraint of 2.3 ka BP to the Neoglacial readvance (Weidick and Bennike, 2007). Radiocarbon ages from proglacial lakes in front of the terrestrial margins of JI

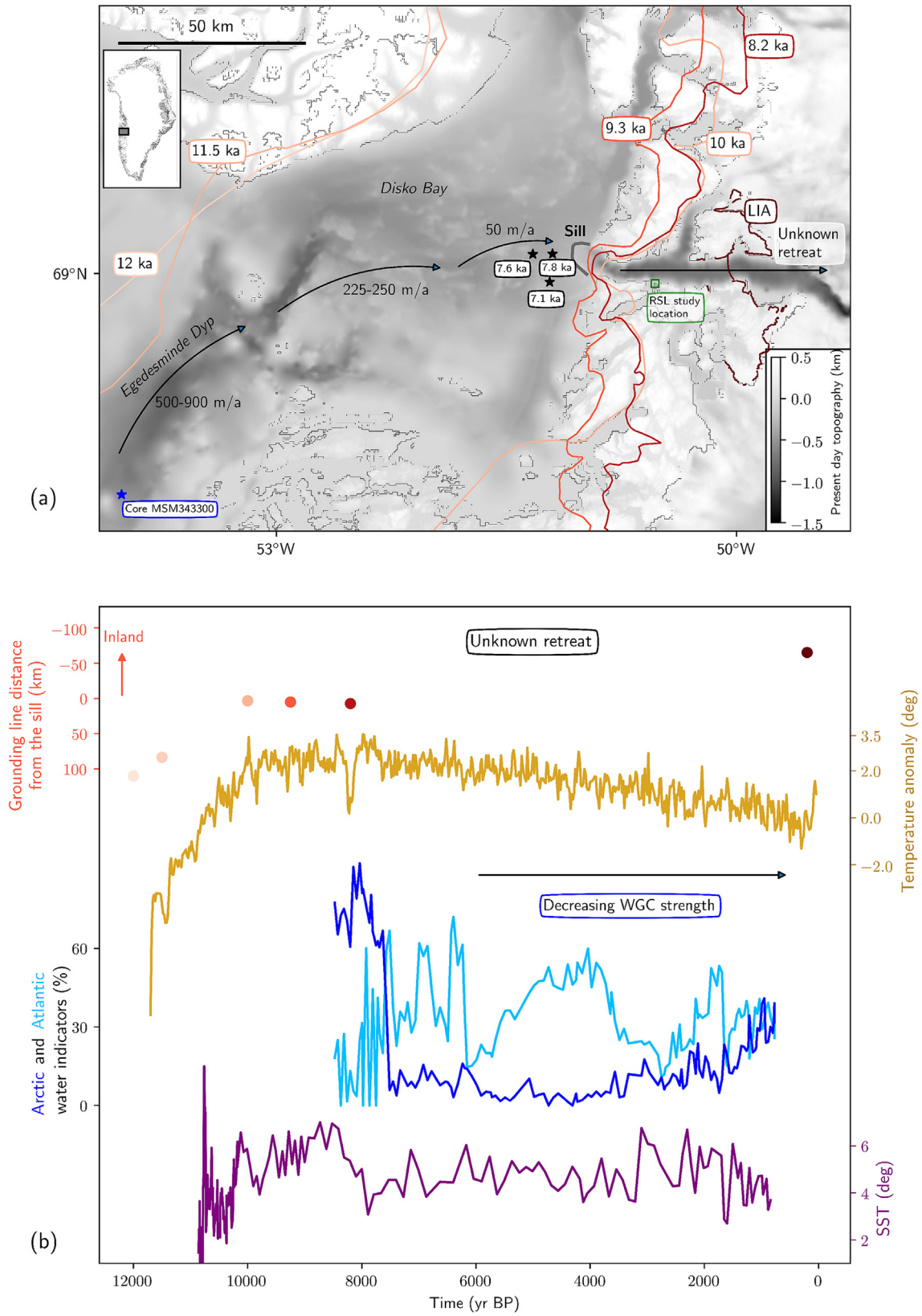

Fig. 1. Summary of the geomorphological evidence of the retreat of JI from Mid- to Late-Holocene, and proxy data showing the evolution of the different forcings: a) Ice front reconstructions are marked with colored lines (Young and Briner, 2015), retreat rates and estimates of the timing of grounding line retreat west of the sill are from Streuff et al. (2017) and Lloyd et al. (2005) (black stars). The location of the core MSM343300 is marked with a blue star, and the location of the RSL study area of Long et al. (2006) is marked with a green rectangle. The greyscale background is the present day bedrock topography and bathymetry from Morlighem et al. (2017). b) Grounding line position in reference to the sill is marked with red dots (colors as in the front reconstructions in panel a), the average Holocene temperature anomaly over Greenland is from Vinther et al. (2009) (yellow line). The Arctic (dark blue) and Atlantic (light blue) water indicators in the West Greenland Current entering Disko Bay from core MSM343300 (Moros et al., 2016), and the initiation of

indicate an asynchronous readvance: the Neoglacial maximum limit was reached already at 2.3 ka BP south of Jakobshavn fjord, but only at 400 a BP north of the fjord (Briner et al., 2010). Results based on a moss chronology from Sikuiui Lake on the Nuussuaq peninsula, approximately 200 km northwest of JI, indicate small advances in local ice caps at 6 ka BP, and distinct advances since 4 ka BP (Schweinsberg et al., 2017). There is little data on the evolution of the marine terminus of JI before 1850 AD, but Wangner et al. (2018) present IRD fluxes from marine sediment cores in front of the sill, indicating that the terminus was grounded 2-0.5 ka BP, and evolved into a floating terminus after 500 a BP.

2.3. Oceanic conditions in Disko Bay

The oceanic conditions in Disko Bay are determined by a combination of glacial meltwaters and the West Greenland Current (WGC). The WGC consists of two main ambient ocean water types: warm and salty Atlantic water, and cool and fresh Arctic water. The present-day water column in the Jakobshavn fjord is stratified into two main water bodies (Beaird et al., 2017). A 150-m-thick cold water layer sits on top, thickening down to 200 m towards the front of JI. This layer is close to the in-situ freezing point and unable to provide heat for substantial melting. The layer below is several degrees warmer, consisting of glacially-modified WGC water. The deep, warm water layer is the water body causing most of the melt, and its inflow into the fjord is regulated by the available space between the cold water layer and the sill bathymetry at the mouth of the fjord (Beaird et al., 2017).

The summer Sea-Surface Temperature (SST) reconstruction from core MSM343300 of waters entering Disko Bay shows three different periods for surface ocean conditions: a relatively warm period at the Early Holocene with July SST's between 5 and 8 $^{\circ}$C, followed by a cooler period at the Mid-Holocene (8–3 ka BP), with July SST's of 4–5 $^{\circ}$C, and finally the Late-Holocene or Neoglaciation warming, when the July SST's rose to 4–6 $^{\circ}$C (purple line in Fig. 1b). Krawczyk et al. (2017) attribute the Mid-Holocene period of cold surface waters to a large amount of glacial meltwater during the summer season. The timing of the onset of this cold period matches with the period of the retreat of JI inland from the sill, supporting large glacial meltwater fluxes as a reason for the surface water cooling.

The deep, warm WGC waters entering Disko Bay were dominated by cold Arctic waters around 8 ka BP, with only sporadic intrusions of warm Atlantic waters, as indicated by the abundancy distribution of benthic foram species (dark and light blue lines in Fig. 1b, (Moros et al., 2016)). After approximately 7.6 ka BP the proportion of Arctic water drops drastically, while the proportion of Atlantic water increases, which causes significant warming of the deep waters. Atlantic water indicators oscillated in highly variable numbers until 2 ka BP, when the proportion of Arctic water started to increase, suggesting the onset of Neoglacial cooling also in deep waters (Perner et al., 2013; Moros et al., 2016). In addition to changes in the WGC composition, at 6 ka BP the Vaigat Strait north of Disko Bay opened, causing the strength of the WGC to decrease steadily throughout the Holocene (Perner et al., 2013) (arrow in Fig. 1b).

From these records we get a rough idea of some of the main changes in the oceanographic setting of Disko Bay during the Holocene. Around 8 ka BP there was a shift to warmer deep water and cooler surface water conditions, and this shift lasted until the Neoglaciation. Moros et al. (2016) do not present a conversion from the benthic foram abundancy to temperature, but Lloyd et al. (2011) propose a translation for Disko Bay for the past century. They find that at 300 m depth an increase from 5 to 15% of the warm water indicators, and a simultaneous decrease of cold water indicators from 45 to 20% corresponds to a 1° increase in temperature. If a similar estimate were to hold for the data in Fig. 1b, it would indicate a temperature increase of roughly 2° at 8 ka BP. However, the transfer function established for the last century should be used with caution. The applicability to data that is several millenia old is uncertain. For example, it is unknown what role the changing currents and the declining strenght of the WGC play.

What is even more significant for the ocean influence on JI, is how much of the warm water in Disko Bay can actually access the grounding line, once it has retreated into the fjord. It is uncertain how well the composition of the water column entering Disko Bay describes the water column in the fjord, particularly during periods of rapid retreat and significant ice discharge. Data indicate that in the present day configuration, temperature changes at intermediate depth in Disko Bay correlate with JI melt rate changes (Khazendar et al., 2019). However, since the depth of the cold surface water layer regulates the deep warm water influx into the fjord, a large flux of glacial meltwater might have caused the surface layer to deepen, as is currently observed in front of the present day JI (Beaird et al., 2017). If the cooling of Disko Bay surface waters after 8 ka BP was due to increased glacial meltwater as JI retreated, it is possible that the cold upper water layer of the fjord may have deepened enough to block the inflow of the warm deep water into the fjord. In this case the fjord would be filled with very cold water, while there would still be significantly warmer deep water in Disko Bay.

3. Model setup

3.1. Ice-flow model

We use the Ice Sheet System Model (ISSM; Larour et al. (2012)), with the two-dimensional Shelfy Stream Approximation (SSA; Morland (1987); MacAyeal (1989)). This stress balance approximation is well-suited to model fast ice streams and regions experiencing significant sliding at the bed. Ice flow follows a nonlinear, isotropic flow law with a stress exponent of 3 (Glen, 1955; Nye, 1957). The model mesh is a non-uniform triangular mesh with a resolution varying from 10 km in the slow-flowing central ice sheet down to 200 m in the fjord and deep trough, where the grounding line is expected to migrate. The grounding line evolves according to the sub-element hydrostatic scheme (Seroussi et al., 2014), and calving front position is tracked with a level set method (Bondzio et al., 2016). We use a sliding law from Budd et al. (1979), with two values for basal friction: a low value of 20 $(\mathrm{s/m})^{1/2}$ for deep areas in the fjord and trough, and a higher value of 50 $(\mathrm{s/m})^{1/2}$, for the rest of the domain. The values correspond to the average values for respective regions obtained from inverting the present day surface velocity (Larour et al., 2012; Seroussi et al., 2013).

The model domain in the inland area corresponds to the present-day drainage area, (Rignot and Mouginot, 2012). However, the domain is extended downstream to include the Holocene extent of the glacier. The ice divide and lateral boundaries are fixed. The bedrock topography is the present day topography from BedMachine v3 (Morlighem et al., 2017); we modified the bed by elevating the sill by 55 m. This change in sill depth is motivated by the results of the spinup calibration, as explained in Section 4.1. The

decreasing West Greenland Current strength in Disko Bay from Perner et al. (2013). SST reconstruction from core MSM343300 (purple line) is from Krawczyk et al. (2017). (For interpretation of the references to color in this figure legend, the reader is referred to the Web version of this article.)

change in sill depth can be explained by the effect of iceberg keel scouring during the Holocene, as has been observed in other fast-flowing marine-terminating glaciers (Wise et al., 2017; Jakobsson et al., 2018). The ice thickness and vertically averaged temperature are initialized from a time-slice at 9.5 ka BP from the GIS deglaciation model by Lecavalier et al. (2014). For simplicity, the ice temperature is kept constant troughout the simulations. We introduce shear margins along areas of steep topographic and velocity gradients, and soften these areas with a damage factor of 0.3, which remains constant in time. The damage factor reduces linearly the ice viscosity, allowing the decoupling of the fast-flowing ice stream from the rest of the domain. This procedure is standard for JI (for example (Van Der Veen et al., 2011; Nick et al., 2013; Bondzio et al., 2017)), and the damage value is a result of the spinup calibration, as detailed in Section 4.1.

3.2. Calving

Ice front migration is implemented using the level set method (Bondzio et al., 2016). In this method the ice front is advected at the front velocity:

$$\mathbf{v}_{front} = \mathbf{v} - \left(c + m_{\text{front}}\right)\mathbf{n}, \tag{1}$$

where $\mathbf{v}$ is the horizontal ice velocity vector, c the calving rate, m_{front} the melting rate at the vertical calving front, and $\mathbf{n}$ the unit normal vector pointing horizontally outward. The calving rate is based on the VonMises calving criterion (Morlighem et al., 2016):

$$c = \frac{\sigma_{\text{VM}}}{\sigma_{\max}} ||\mathbf{v}||, \tag{2}$$

where σ_{VM} is the von Mises tensile stress, $\sigma_{\max}$ the maximum allowed stress in the ice, and $\|\mathbf{v}\|$ the magnitude of the horizontal ice velocity. In this formulation, calving is always present, but the ratio of σ_{VM} over the threshold $\sigma_{\max}$ determines whether the ice front advances along the ice flow direction or retreats in the opposite direction. In other words, when the stress state in the ice is high enough, the ice front retreats. The model enables the development and maintenance of a floating tongue, since the ice front and grounding line evolve independently from each other, and $\sigma_{\max}$ has a different value depending on if the front is floating or grounded. Present-day values of the threshold for JI were calibrated in Bondzio et al. (2017) to oscillate between summer and winter values of 60–600 kPa for floating ice, and approximately 100 kPa to 4 MPa for grounded ice. For our model setup, we calibrate the values for the calving parameters within these ranges during the spinup (see Section 4.1), and find that suitable constant values for the Holocene are 300 kPa for floating ice and 1 MPa for grounded ice.

3.3. Forcings

3.3.1. Surface mass balance

Since the Mid-Holocene climate of coastal areas in Greenland is largely unknown, changes in surface mass balance (SMB) are represented by imposing variations in the equilibrium line altitude (ELA) (Helsen et al., 2012). The strength of this method is that the ELA implicitly accounts for changes in all processes contributing to the SMB, which might not be possible to include in a SMB-model applicable on long time scales. The SMB computed for every point is:

$$SMB(\mathbf{x}, t) = b(\mathbf{x})(S(\mathbf{x}, t) - ELA(t)), \tag{3}$$

where $b(\mathbf{x})$ is the vertical SMB gradient for each point, assumed to be time independent, $S(\mathbf{x}, t)$ is the ice surface elevation at time t, and $ELA(t)$ is the equilibrium line altitude at time t. The vertical SMB gradients $b(\mathbf{x})$ are calculated from a reference SMB. As the reference SMB, we use a regional MAR climate generated from a pre-industrial global NorESM boundary climate, as in Plach et al. (2018). To avoid unrealistic values, the computed SMB is capped between at 0.9 m ice eq./a and −4 m ice eq./a.

Air temperature gives an indication of ELA, but since the ELA also depends on accumulation, the exact ELA values for JI during the Holocene are unknown. Weidick and Bennike (2007) measured the ELA of the JI catchment over three years in the 1980's, and find that values range from 1000 to 1200 m. The ELA of our reference SMB is 1300 m. From this we infer that the Holocene Climate Optimum (HCO) maximum value, ELA_{HCO}, was likely above, and the LIA minimum ELA, ELA_{LIA}, below the observed values. We calibrate ELA_{HCO} during the spinup (for details see Section 4.1, and Fig. 3), and test a range of values for the ELA_{LIA} in the forward runs, as described in Section 4.2. Humlum (1987) estimate the ELA_{LIA} minimum to be 200 m below present day on the nearby Disko Island. We choose a range of 600–1000 m, to capture the uncertainty.

3.3.2. Submarine melt

The ocean forcing in our model is prescribed through two different melt-rates at the ice front below sea level. First is the submarine melt rate, m_{sub}, applied at the base of the floating ice, that is, how much ice melts in the vertical direction. The other melt rate is the frontal melt rate, m_{front}, included in the front velocity formulation (Eq. (1)), which causes melting perpendicular to the vertical ice front and in the opposite direction to the ice flow. This frontal melt rate is different from the submarine melt rate, since it is a parameter which combines effects not included in the calving rate, such as undercutting and seasonal frontal melt caused by meltwater plumes. For simplicity, the frontal melt and submarine melt are assumed equal throughout the study.

The benthic foram data from Disko Bay indicates that there was a shift to warmer conditions around 8 ka BP, which corresponds to the start of our transient runs. Therefore, we calibrate a low melt rate value for the spinup, and a high HCO melt rate starting from 8 ka BP in the transient runs (Fig. S6). We test a range of simplified ocean forcings in the transient runs, as described in Section 4.2. We test a range of low melt rate values for the LIA, down to 10 m/a, which corresponds to values found today in marine terminating glaciers in cold oceanic settings in Northern Greenland, such as Peterman Glacier, or 79 North Glacier (Wilson et al., 2017). Bondzio et al. (2017) used submarine melt rates ranging from 270 to 540 m/a for their model of JI in the recent decades, and our calibration indicates that 600 m/a gives unrealistically high retreat rates, thus limiting the higher end of tested melt rate values.

3.3.3. Relative sea level

The relative sea level changes up to 50 m in our model domain during the studied time period from 8 ka BP to the LIA (Long et al., 2006; Lecavalier et al., 2014). The largest changes take place at the edges of the GIS, where the overall impact is a decrease in the relative sea level, while in the interior of the ice sheet the relative sea level increases (Long et al., 2006; Lecavalier et al., 2014). We assume that the geometry of JI is dominated by sufficiently steep features, such as the trough and the fjord, that small changes in the bed slope due to postglacial uplift are negligible. However, changes in relative sea level are significant at the sill, where floatation affects the initiation of the glacier's retreat.

Since we use a regional model, computing relative sea level changes is not feasible because we lack the impact of ice mass changes outside of our domain. Thus, we keep the bed elevation in our model constant, and force the sea level with the relative sea level from the Greenland deglaciation model by Lecavalier et al. (2014). This modelled relative sea level matches relatively well with a relative sea level reconstruction from sediment cores from lakes adjacent to Jakobshavn fjord (Long et al., 2006). The modelled relative sea level for all grid points in the fjord are shown in light grey, and reconstructed relative sea level in blue in Fig. 2. The relative sea level forcing is a field that is updated at 500 year intervals in the forward runs. During the spinup, however, all forcings are kept constant at their initialization value, which causes a discontinuity in the relative sea level when shifting from the spinup run to the forward runs (see dark grey in Fig. 3.3.3). The spinup is discussed further in Sections 4.1 and 6.

4. Experimental setup

The purpose of this study is to investigate the unknown Mid-Holocene retreat and minimum extent of JI. First, a model of the glacier is constructed and run as a spinup with constant forcings until the ice front is stable. The end of the spinup is considered to correspond to the ice configuration at 8 ka BP, and the model is run forward to the LIA with different transient forcings.

4.1. Spinup

We initialize the model using ice surface, extent, and relative sea level at 9.5 ka BP from Lecavalier et al. (2014). To create a spinup for the Mid-Holocene, we assume that the ice front was stable, the ice stream was grounded on the sill, and the volume did not fluctuate much. The spinup is run until the model reaches a stable front position, corresponding to the locations of the dated moraines at 10–8 ka BP (Fig. 1), (Young and Briner, 2015), and the grounding line remains grounded on the sill. The spinup is run with constant forcings, even though we know that there were some minor ice front fluctuations, likely ice volume fluctuations, and the relative sea level was changing during this time (Lecavalier et al., 2014; Young and Briner, 2015). However, none of these changes appear to have caused the grounding line to fluctuate significantly from the sill, so for the purpose of our model, these effects are considered negligible. There might have been a general trend of either thinning or thickening of ice volume, but we assume that the trend was slightly towards decreasing due to the warm HCO.

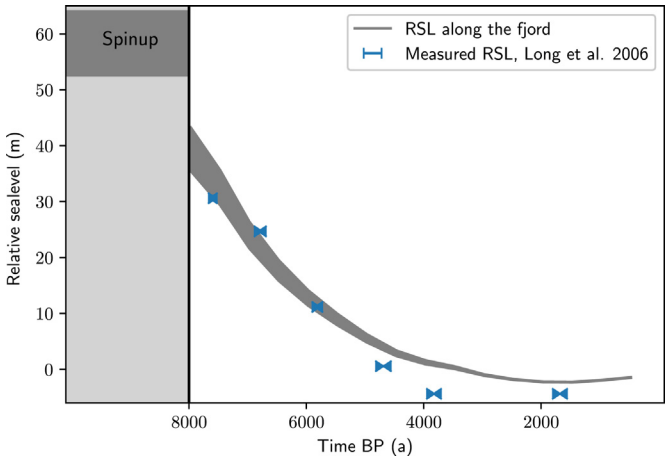

Fig. 2. Relative sea level at all grid points around the fjord during the forward runs (grey), adapted from Lecavalier et al. (2014). Relative sea level at all points around the fjord during spinup are represented as grey on light grey background. Observed relative sea level next to the fjord (blue markers) (Long et al., 2006). (For interpretation of the references to color in this figure legend, the reader is referred to the Web version of this article.)

During the spinup, we find a range of acceptable values for each of the unconstrained parameters: ELA_{HCO}, sill depth, shear margin softening, basal friction, calving parameters, and the submarine melt rate. The main constraint of the spinup is that both the terrestrial ice margin and the grounding line should remain stable for at least two millenia. Parameters are deemed reasonable, if they fulfill the no-retreat condition of the spinup. Some parameters, such as the sill depth and ELA_{HCO} value are connected, and we find several stable combinations. The submarine melt rate is kept low during the spinup to allow the ice surface to reach equilibrium, which is consistent with the high concentration of Arctic water in the WGC before 8 ka BP (Fig. 1, (Moros et al., 2016)).

4.2. Transient runs

The forward runs with transient forcings start from the end of the spinup run, assuming it represents the ice configuration at 8 ka BP. Parameters remain the same as in the spinups, except the ocean melt rate, which is assumed to increase to a calibrated high melt rate value, and the calving parameter, which is also recalibrated. The different transient atmospheric and oceanic forcings are tested both separately and combined. First, we run single forcing sensitivity experiments, where we keep either atmospheric or ocean forcing constant at the HCO level, while the other forcing is transient, in order to study the response of the model to different forcings. We then use combinations of cool forcings to constrain the Holocene minimum extent of the glacier, by testing what is the farthest inland position that the grounding line can reach, while still being able to grow back to its LIA extent within the expected timing. All model runs with respective acronyms and forcings are described in Table 1.

We test three different types of atmospheric forcings. Since the general trend of Holocene climate cooling in Greenland after 8 ka BP (Fig. 1) is close to linear (Vinther et al., 2009), the default atmospheric forcing is a linear ELA decrease (LE). The extreme atmospheric forcing that is meant to test the limits of the model is an early stepwise decrease of the ELA directly to the LIA value (SE). Finally, the variable ELA forcing directly follows the variations of the Holocene temperature anomaly curve (VE) (yellow line in Fig. 1). In runs testing the model sensitivity to ocean forcing, the ELA remains constant at the HCO level (CE).

Ocean forcing is created by varying the ocean melt rate in time. At the start of each forward run, the melt rate is increased to a high HCO value to initiate retreat from the sill. This melt rate values are calibrated for our model setup, representing the shift in ocean conditions indicated by the benthic foram data at 8 ka BP (blue lines in Fig. 1). The ocean forcing is either constant, at the high HCO value (CM), or a stepwise decrease in the melt rate to simulate ocean cooling after the high HCO conditions (SM). We apply this stepwise change at different times and investigate the effect on the retreat history of JI.

5. Results

5.1. Spinup run

First, we run a spinup model from the initial setup with constant forcings. During the spinup, the terrestrial ice margin retreats from the initial ice extent close to the location of the reconstructed ice margins for 10–8 ka BP (Fig. 3a). The grounding line of the ice stream retreats from the initial extent to the sill, which is a pinning

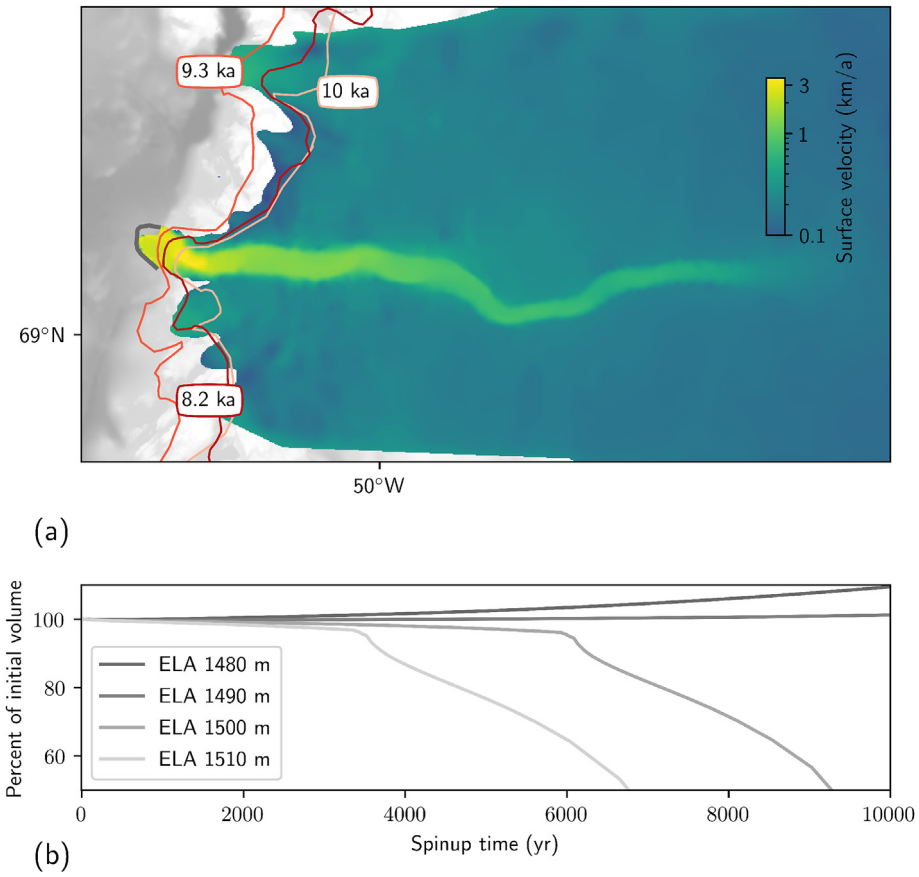

Fig. 3. Result of the spinup: (a) surface velocity and ice configuration at the end of the spinup (color scale), in relation to the reconstructed terrestrial margins (red lines) and the sill (grey line); (b) Ice volume evolution in spinup runs with different ELA_{HCO} values. (For interpretation of the references to color in this figure legend, the reader is referred to the Web version of this article.)

Table 1
Names and forcings used in model simulations.

Model name	ELA forcing type	ELA_{LIA}	Marine forcing type	Melt rate
LE_CM	Linear	600 m, 800 m	Constant	500 m/a
SE_CM	Step at 7700 BP	600 m, 800 m, 1000 m	Constant	500 m/a
CE_SM	Constant	1500 m	Step at 7700 BP	100 m/a, 150 m/a
LE_SM	Linear	1000 m	Step at 7600 BP	100 m/a
SE_SM	Step at 7500 BP	800 m	Step at 7500 BP	10 m/a
VE_SM	Variable	1000 m	Step at 7600 BP	50 m/a

point in the bathymetry. However, the grounding line is prone to retreat further inland from the sill, and is sensitive to changes in model parameters. In order to enable the ice stream to extend to the sill, further out than the rest of the glacier, the shear margins need to be softened. Including shear margin softening allows the ice stream grounding line to stabilize on the sill, while the terrestrial ice margin retreats to the topographic high, 20 km inland from the sill. Without softening, the modelled marine terminating front is prone to retreat in line with the terrestrial margin due to internal stresses that do not allow the decoupling of the terrestrial and marine margins (Bondzio et al., 2017). This would cause the grounding line of the ice stream to retreat inland from the sill on to the deep retrograde bed, from where the marine ice sheet instability will keep the ice stream retreating even further inland.

In addition to shear margin softening, the tendency for rapid retreat creates sensitivity to other unconstrained parameters. The values used for the ELA_{HCO}, sill depth, ice temperature, basal friction, ocean melt rate during spinup, and calving parameters are constrained by the criteria that the ice margin and grounding line must be located close to the reconstructed margin. ELA_{HCO} is the most significant of these unknown parameters affecting stability of the glacier. Once the ice edge has retreated to the expected extent, the ice volume still changes, either decreasing or increasing, depending on the ELA_{HCO} value (Fig. 3b). The difference is characterized by a sharp transition at a certain threshold ELA value.

The parameter selection of the spinup is further illustrated in Fig. 4. The figure shows the range of sill depths and ELA_{HCO} values tested. Runs are limited by three conditions: the grounding line must remain stable on the sill for at least 2000 years; total ice volume must decrease; and the ice cannot thin so much that it starts floating in the deep trough inland. We see that the range of acceptable sill depths is relatively large, while the acceptable ELA_{HCO} range is constrained around 1500 m. A similar testing procedure is applied to all unconstrained parameters. All parameter values used in both the spinup and the transient runs are listed in Table S1.

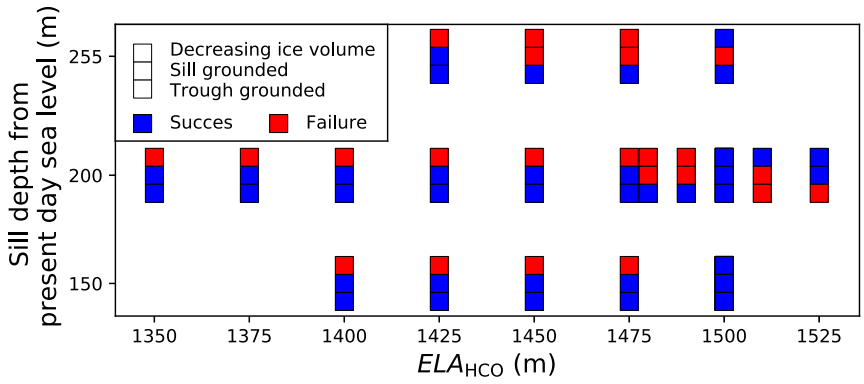

Fig. 4. Visualisation of the spinup calibration with respect to sill depth and ELA_{HCO}. Spinup is ran with each combination, and pass/fail of three conditions, presented in Section 5.1, is indicated with blue/red. (For interpretation of the references to color in this figure legend, the reader is referred to the Web version of this article.)

5.2. Transient runs, 8 ka BP to the LIA

Transient runs start from the ice configuration of the spinup (Fig. 3a). The retreat during the transient run is initiated by a sharp increase in the melt rate to cause ungrounding from the sill, and run forward 8000 years (calibration of the melt rate increase is presented in Figures S5 and S6). The calving parameter σ_{max} is recalibrated to prevent unrealistically rapid retreat of the ice front. During the forward runs either ELA, melt rate, or both evolve through time, in addition to the relative sea level (see Fig. 5b and c). Results are presented as grounded area extent in reference to the grounded area at the end of the spinup run. Since the inland extent of the domain is kept constant, a change in the grounded area is the sum of changes in the terrestrial ice margin and the grounding line. The terrestrial margin and grounding line do not always evolve synchronously, in which case we study their evolution separately in plan view and along a flowline.

5.2.1. ELA and ocean melt sensitivity tests

In our first set of forward runs we test the sensitivity of the model to changes in one forcing at a time. We test linear and stepwise decrease of the ELA, and a stepwise decrease in ocean

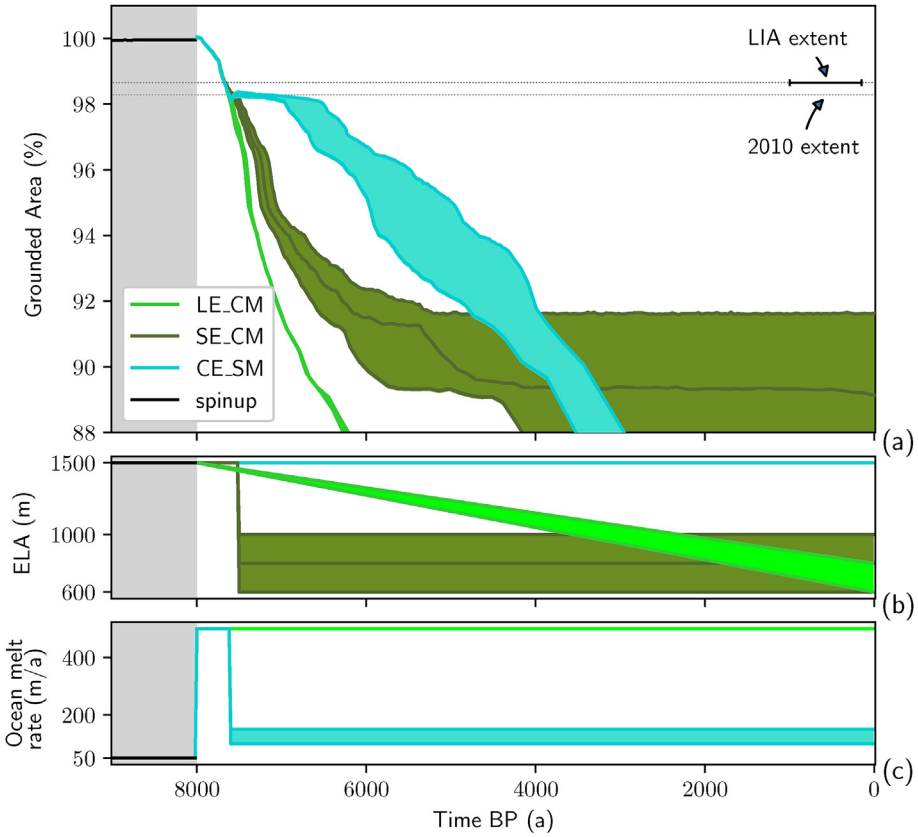

Fig. 5. Grounded area evolution (a) of JI forced with different ELA or ocean melt rates, and the respective atmospheric (b) and ocean (c) forcings through time. Each forcing is tested for a range of different end values: linear ELA decrease (pale green), stepwise ELA decrease (dark green), and stepwise ocean melt decrease (pale blue). Dark and light green lines overlap in (c). (For interpretation of the references to color in this figure legend, the reader is referred to the Web version of this article.)

melt from their respective high values at the start of the transient, each with a range of end values. Runs with linearly decreasing ELA (LE_CM, light green range Fig. 5), show a drastic decrease in the grounded area, indicating that both the terrestrial ice margin and grounding line retreat rapidly, far inland from the LIA and the present day extents of the glacier. Runs with a stepwise decrease in ELA (SE_CM, dark green range on Fig. 5), retreat similarly to LE_CM for the first 1000 years, showing only slightly slower retreat following the step in the ELA at 7.7 ka BP. After 7 ka BP, the retreat slows down and the grounded area stabilizes with the lowest ELA_{LIA} values. However, the stable ice configuration is much smaller than the LIA or the present day ice extent. With the higher ELA_{LIA} values, the grounded area does not stabilize, but keeps on retreating.

With all models, the 10-year-average retreat rate of the grounding line reaches up to 1000 m/a in the rapidly deepening sections of the topography inland of the sill and at the start of the trough. On the terrestrial margins close to the fjord, retreat rates can reach up to 500 m/a, following the rapid retreat of the marine terminus.

Runs with a stepwise decrease in ocean melt rate at 7.7 ka BP show an instant slowdown in the grounded area retreat after the step decrease in melt rate takes place (CE_SM, pale blue range in Fig. 5). However, this slowdown lasts for approximately 1000 years, until the retreat continues due to continuing volume decrease (Fig. S1). This result shows that the grounded area reacts to changes in melt rate immediately, even if eventually the volume decrease due to thinning forces retreat. All the single forcing runs show retreat while either ELA or ocean melt have the high HCO value, and only the most drastic cooling of the climate can eventually stop this retreat. Furthermore, none of the runs show grounded area increase during the 8000 years of the model run, which means there is no readvance of either the grounding line or the terrestrial margins, when only either atmospheric or oceanic changes are applied.

5.2.2. The Holocene minimum extent

In the second set of forward runs we test combinations of transient ELA and melt rate forcings in order to create a model that will readvance to reach the LIA extent. Fig. 6 presents grounded area evolution and forcings of two different runs (LE_SM and SE_SM) that show grounded area increase. LE_SM (purple lines in Fig. 6) is forced by a linear ELA decrease and a stepwise decrease in ocean melt rate. SE_SM (pink lines in Fig. 6) has a stepwise cooling in both the atmospheric and ocean forcing, and the final values for both are cooler than the ones reached at the end of LE_SM. We note that these steps in forcings take place later in SE_SM, at 7.5 ka BP, whereas in LE_SM they take place at 7.6 ka BP. In Fig. 6 the initial rapid grounded area retreat of both models is similar, until the step change in melt rate in LE_SM is applied. After the step change, grounded area in LE_SM rebounds slightly, before decreasing slowly to the Holocene minimum extent at 6–5 ka BP. Since SE_SM has step changes 100 years later in both forcings, the grounded area continues to retreat rapidly at the same rate for the extra 100 years before the steps take place. Since SE_SM has a step cooling in both forcings, the initial quick rebound of the grounded area after the step is larger than for LE_SM. The grounded area increase of SE_SM continues throughout the model run due to the cool forcings, but this readvance slows down in time, and does not reach the present day extent by the end of the simulation.

Fig. 7 presents the frontal evolution at 100-year-intervals of both LE_SM and SE_SM in plan view and along a flowline, giving more insight on the spatial evolution of the margins and on the grounding line position separately. Fig. 7c shows that in LE_SM the grounding line retreat stops as the step change in melt rate at 7.6 ka BP is applied, before a bump in the bathymetry 60 km from the sill. The grounding line then readvances immediately, explaining the small rebound of grounded area in Fig. 6, before settling close to the LIA location. Fig. 7a shows that the minimum extent at 6–5 ka BP is due to the sustained retreat of the terrestrial margins, which shifts to readvance only when the atmospheric focing is cold enough to build up ice volume again (Fig. S2).

In SE_SM the grounding line retreats beyond this bump at 60 km, and remains in the deep trough for the rest of the run, despite the very cool forcings of both atmosphere and ocean (Fig. 7d). The grounded area evolution of SE_SM in Fig. 6 shows increase immediately after the step change at 7.5 ka BP, but Fig. 7b and d shows that this increase is, in this case, caused by the terrestrial margins, not by the grounding line advance. The advance of the terrestrial margins eventually stops since they cannot advance further before the marine part also advances, and the fjord becomes ice filled again.

Fig. 8 presents a case with a realistic atmospheric forcing and stepwise ocean cooling, VE_SM, where the ELA varies following the variations of the Greenland temperature anomaly (yellow line in Fig. 1b). The general shape of the evolution of the grounded area is similar to the evolution of LE_SM (pink line in Fig. 6): the initial retreat is rapid, following a slowdown after the step decrease in the melt rate, and the Holocene minimum extent is slightly below the present day extent and reached at 5 ka BP. However, there are some differences due to the higher ELA oscillations directly after 8 ka BP and through the Mid-Holocene. Due to the higher ELA values, VE_SM needs a lower melt rate pulse to initiate retreat from the sill, which causes the initial retreat to be slower than with the higher melt rate of LE_SM. The higher ELA oscillations also mean that VE_SM requires a lower step than LE_SM in the melt rate to enable readvance. Although the minimum extent in grounded area is reached at 5 ka BP, the grounded area remains low until 3 ka BP, when the readvance starts to pick up, while the atmospheric forcing cools. The variability of the atmospheric forcing translates to variability in the evolution of the terrestrial margins and thus to the total grounded area. However, the grounding line is not impacted by these short time scale variations of atmospheric forcing (Fig. S4).

All the runs show that even with cold forcings, the readvance rate is slow, and grounding line readvance is particularly slow, except for stepwise changes in the ocean forcing. All the runs indicate that the position of the grounding line at the time when the stepwise decrease in ocean melt is applied is crucial to the future evolution of the glacier, as is seen when comparing Fig. 7a and c to 7b and 7d. From the slow readvance follows that the grounding line could not have retreated into the trough beyond the bump at 60 km during the Holocene, since it would not have had the time to readvance to the LIA extent (Fig. 6).

6. Discussion

In this study we use a high-resolution 2D ice flow model to simulate the evolution of JI from the Mid-Holocene to the LIA. This is the first time a high resolution regional model is used to study the grounding line migration of JI over the past millenia. Guided by proxy records of Holocene climate change on Greenland, several forcing scenarios are tested in order to find a combination recreating the observed pattern of glacier retreat and readvance. By requiring a readvance to the observed LIA extent, our simulations constrain the Holocene minimum extent of JI close to the present position of the glacier.

We find that, during the Holocene, the grounding line of JI could not have retreated beyond the bedrock bump close to the present day calving front. There is no geomorphological evidence for the retreat of the grounding line during the Mid-Holocene, and the

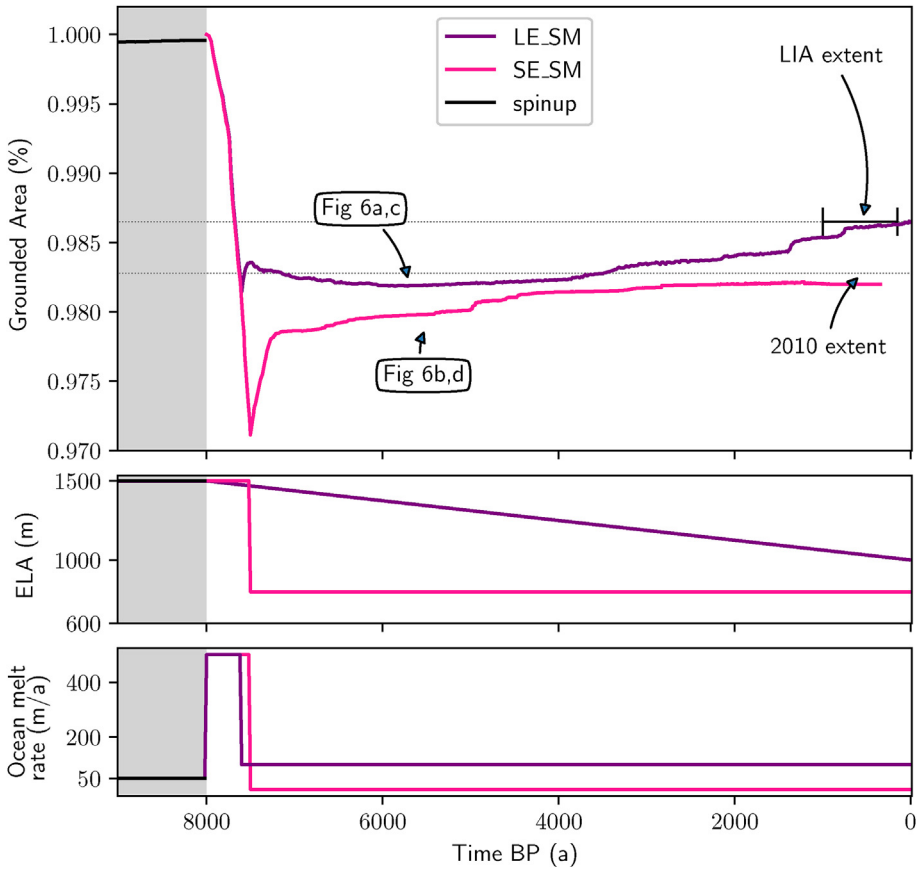

Fig. 6. Grounded area evolution (a) of JI in different combined forcing runs: LE_SM (purple) and SE_SM (pink), and the respective atmospheric (b) and ocean (c) forcings through time. (For interpretation of the references to color in this figure legend, the reader is referred to the Web version of this article.)

previous modelling studies show either a retreat as far as 100 km inland from the present day extent (Tarasov and Peltier, 2002; Nielsen et al., 2018), or no retreat from the sill at all (Simpson et al., 2009; Lecavalier et al., 2014; Cuzzone et al., 2019). For the terrestrial margins we find that the retreat was on average less than 10 km inland from the present day margin. Our result is close to the result of Weidick et al. (1990), who estimated a 15 km retreat of the terrestrial margins of JI from the present day extent, based on dated archaeological finds transported by the ice. Our simulated minimum extent took place between 6 and 4 ka BP. This is in line with Briner et al. (2010) who studied proglacial lakes in front of the present day terrestrial margin of JI, and concluded that the minimum extent took place between 6 and 5 ka BP. Nielsen et al. (2018); Tarasov and Peltier (2002) model a readvance close to the JI catchment, but the timing of the minimum extent is at the HCO around 8 ka BP, too early compared to the dated ice margin reconstructions (Young and Briner, 2015). The differences between our model results and previous modelling studies highlight the importance of high model resolution capturing the ice streams, detailed topography, and grounding line evolution (Greve and Herzfeld, 2013; Cuzzone et al., 2019; Seroussi et al., 2014).

By calibrating the model using the reconstructed and observed frontal positions, we are able to find the combination of atmospheric and marine forcing required to create the retreat-readvance pattern of JI during the Holocene. Ocean cooling is needed to stop the retreat of the grounding line, and atmospheric cooling is needed to increase the ice volume, allowing the LIA readvance. The necessity of ocean cooling is clear in the combined forcing runs (Fig. 6), and similar behavior is observed when applying the proxy-based, variable atmospheric forcing (Fig. 8). Due to the fjord setting with a retrograde bed, the grounding line is extremely sensitive to changes in ocean melt, and a significant melt rate decrease is needed to stop the retreat of the grounding line. This sensitivity is in line with the marine ice sheet instability of marine terminating glaciers on retrograde bed slopes (Schoof, 2007; Gudmundsson et al., 2012; Jamieson et al., 2014; Nielsen et al., 2018). However, one can also note that most of the stable positions of the glacier (LIA and present day) coincide with the upstream end of embayments of the fjord. This is in line with the studies of Åkesson et al. (2018); Steiger et al. (2018) on the stabilizing effect of the lateral geometry of fjords. Unfortunately, our study with a complex fjord geometry cannot disentangle the separate effects of the depth and width of the fjord. Our finding of the necessary forcing combination is also in line with the assumption that SMB drives the large scale fluctuations of the ice sheet (Huybrechts, 2002; Simpson et al., 2009), since we show that atmospheric cooling is necessary to create readvance. However, atmoshperic cooling is not sufficient to create readvance in our setup if ocean conditions are not cold enough.

We find that ocean cooling is necessary to prevent retreat into the deep trough inland from the fjord. This means that the cooling must have taken place relatively soon after the initiation of the retreat. Based on Atlantic water benthic foram indicators from core MSM343300, there is no clear evidence of such a persistent cooling (light blue in Fig. 1b). However, the fjord is separated from Disko Bay by a relatively shallow sill, with only 200 m access into the fjord in our setup. In the present day Jakobshavn fjord the cold surface water layer grows deeper closer to the front, reaching approximately 200 m just a few km from the front (Beaird et al., 2017). We

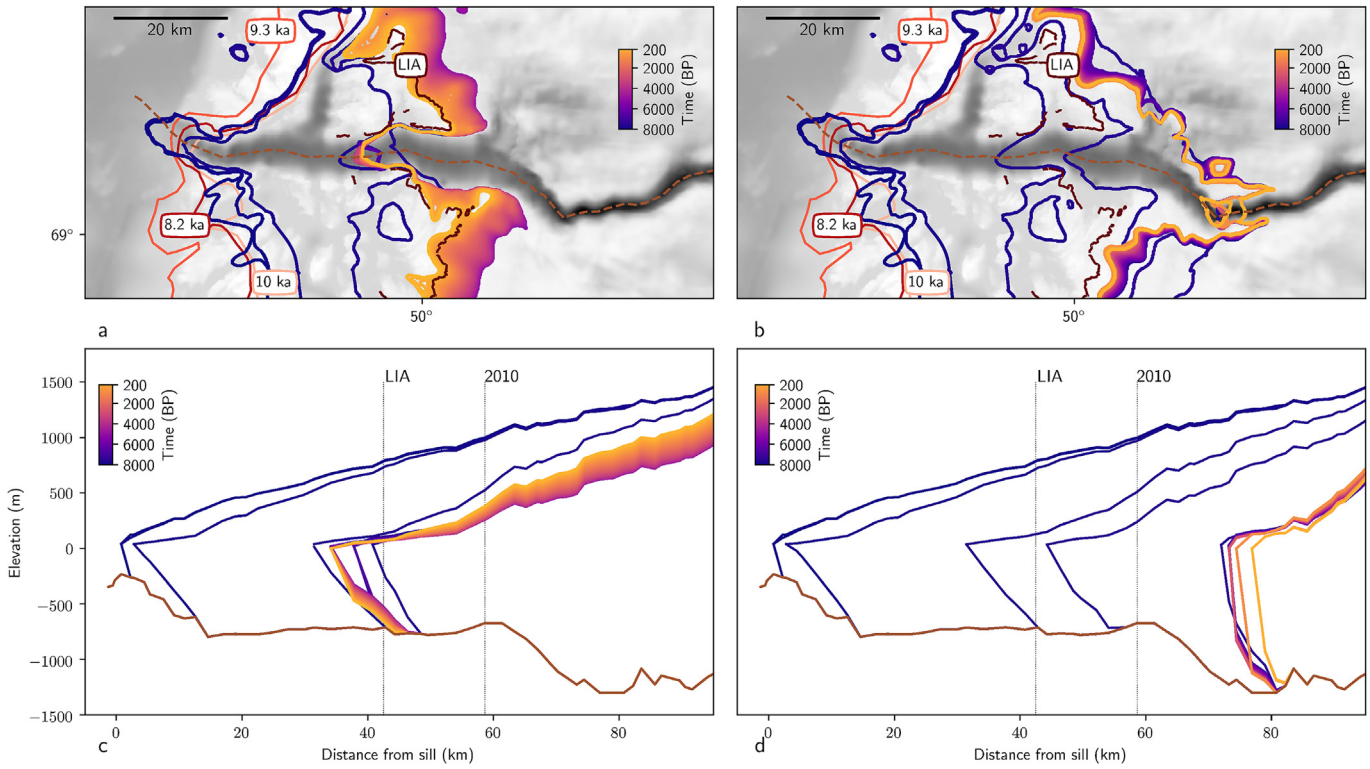

Fig. 7. Terrestrial ice margin and grounding line evolution of JI at 100-year intervals in two model runs, LE_SM and SE_SM. a,b) plan view of LE_SM and SE_SM respectively. c,d) LE_SM and SE_SM respectively along a flow line. The flowline is the brown dashed line on panels (a,b). Ice margin reconstructions (red lines) from Young and Briner (2015). (For interpretation of the references to color in this figure legend, the reader is referred to the Web version of this article.)

consider it likely that input of glacial meltwater, due to rapid retreat of the glacier could have sufficiently deepened the fresh water layer in the fjord, blocking the warm deep waters from accessing the fjord over the sill. This would decrease the melt rate at a crucial phase of the retreat.

We attribute the retreat from the sill at 8 ka BP to ocean warming, rather than to thinning due to a warm atmospheric forcing. We base this on the observed abrupt shift in ocean conditions at this time (Fig. 1b). The ice volume was not monotonously decreasing, and possibly not even thinning, for the millenia before the retreat. This can be seen from the order of the reconstructed moraine fronts. The 9.3 ka BP front is to the west of the 10 ka and 8.2 ka fronts, and for most of the study area, the 10 ka BP front is found further inland (Fig. 1). In other areas, along the Western Greenland ice margin, the retreat rate shows no indication of a pause between 10 and 8 ka BP, and the retreat pattern is relatively linear, and dominated by thinning (Lesnek and Briner, 2018). This supports the assumption that the abrupt retreat at JI was due to changes in ocean conditions. When running additional sensitivity experiments, testing if the retreat from the sill is due to overall thinning of the glacier, we find that a readvance in our setup requires that the glacier has not thinned too much on the terrestrial areas. This supports our assumption that ocean warming is required to trigger the retreat.

We find that the simulated retreat rates from the sill to the middle of the fjord are on the order of 300 m/a, averaged over 100 years. At approximately 30 km inland from the sill, the retreat rate in our model reaches 1000 m/a, when the grounding line passes a wide section of the fjord. These rates are within the range of what is found for the paleo-predecessor of JI in Egedesminde Dyp (Streuff et al., 2017). Furthermore, our modelled Mid-Holocene retreat rate is of the same order of magnitude as the observed present day terminus retreat. From 2006 to 2009, following the disintegration of the floating tongue, the terminus of JI retreated at a rate of 600 m/a (Joughin et al., 2012). Since 2009 the retreat has slowed down, and even turned to a readvance (Khazendar et al., 2019). Our modelled retreat rates might have been enhanced by the sliding law: we use Budd et al. (1979), which gives the fastest sliding for both retreat and advance (Brondex et al., 2017). While other sliding laws exist, they would enable less retreat over the Holocene, as they require a longer time to retreat and readvance. Choosing the fastest sliding law gives us an upper limit on the extent of the retreat and the estimated inland location of JI grounding line.

The readvance of the grounding line is significantly slower than the readvance of the terrestrial margins under the climate forcing in our model setup for JI. As the climate is cooled, the terrestrial margins advance rapidly. This is because small changes in ice thickness can directly translate into changes at the terrestrial margins. However, for the marine grounding line to readvance, the ice needs to thicken sufficiently to exceed floatation at the grounding line, while at the same time ice loss due to calving and melt at the front continues. In theory, a floating ice front can readvance at ice flow velocity, limited only by calving and lateral friction. Our results show a floating ice shelf persisting throughout the runs (Fig. 7c and d), but due to the simple depth-independent oceanic forcing and constant calving treshold, it is unlikely that the modelled evolution of the floating shelf is very accurate. The triangular shape of the shelves is due to the melt rate being constant with depth, although the water column in the fjord was likely stratified, as it is at present (Beaird et al., 2017). Wangner et al. (2018) find that the sediment record from Disko Bay in front of the sill indicates a vertical calving front rather than a floating shelf from 2 ka BP to 0.5 ka BP.

During the spinup we found that shear margin softening is

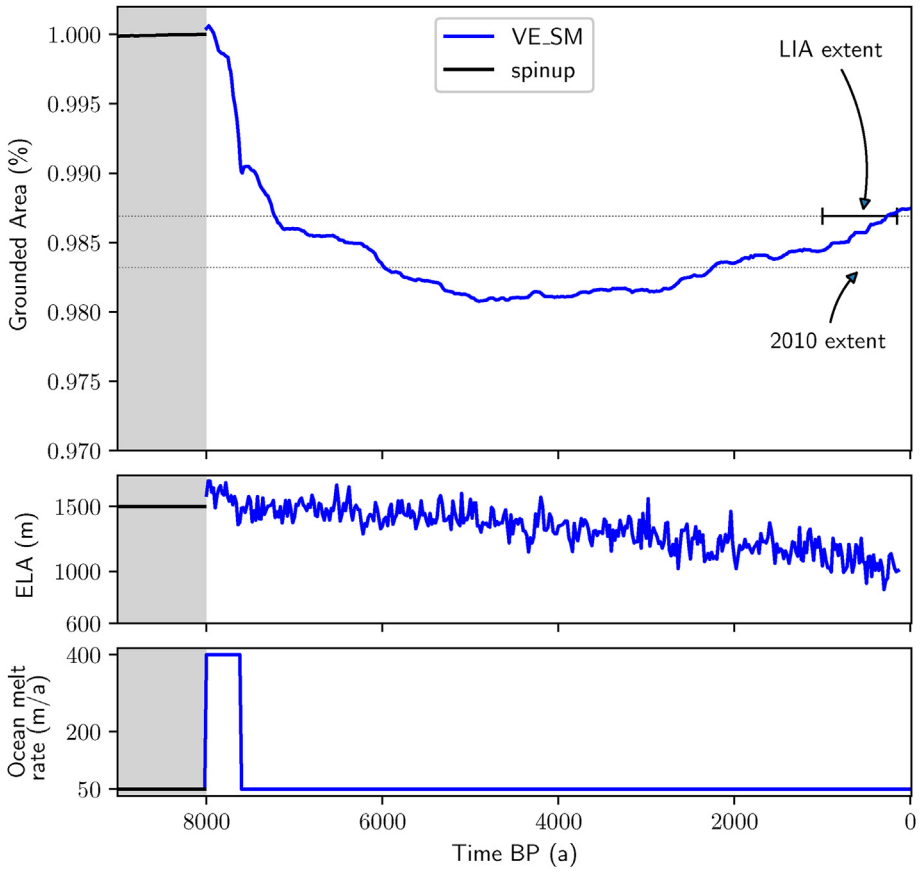

Fig. 8. Grounded area evolution (a) of JI in a combined forcing run, VE_SM, with variable climate forcing, and the respective atmospheric (b) and ocean (c) forcings through time.

needed in order to create the shape of the ice front, as given by the reconstructions (Fig. 3). Shear margins need to have significantly softer ice in order to allow the ice stream to be grounded on the sill, approximately 20 km in front of the terrestrial ice margin. In part, this shear margin softening is needed because the model is 2D and not thermomechanically coupled. Thus, the model lacks softening due to frictional heating, which explains partly the need for shear margin softening. However, in a thermomechanically coupled 3D model for the present day JI (Bondzio et al., 2017), it was also necessary to add shear margin softening to be able to replicate recent fluctuations of the glacier. This indicates that to accurately represent fast flowing glaciers and ice streams such as JI, shear margin softening is required in 2D models, and possibly also in 3D models, suggesting that the softening is not explained by frictional heating alone. Our finding matches also with previous studies, suggesting that shear softening is required to match the observed flow pattern of JI (Vieli and Nick, 2011; Joughin et al., 2012; Nick et al., 2013).

The spinup is run with constant forcings corresponding to a period when the ice was relatively stable. Several unconstrained model parameters are calibrated during the spinup, constrained by the estimated front location and stability of the glacier at the mouth of the fjord. Since the reconstructed front locations show relative stability of the terrestrial ice margin, and sediment cores indicate that the ice stream was grounded on the sill at 10–8 ka BP, we see no reason to doubt our assumption. However, we know that the relative sea level was changing during this time. This causes the relative sea level to drop discontinuously at the start of the forward run (Fig. 3). This drop creates extra stability of the grounding line at the start of the forward runs, due to a decrease in water depth at the sill, which we compensate by increasing the ocean melt rate at the HCO. Thus, the suitable combination of the HCO ocean melt rate, the ELA, and sill depth that creates a retreat from the sill depend on our model setup. Given that the exact values for the melt rate, ELA and sill depth are unknown, any combination of these creating a similar glacier evolution is valid to initiate retreat from the sill. Changing the relative sea level has no effect once the grounding line retreats into the fjord, as changes in sea level are small compared to the depth of the fjord.

Assuming there has been active erosion by iceberg scouring, we have raised the sill at the mouth of the fjord by 55 m compared to the present day bathymetry. We found that some increase is necessary to stabilize the grounding line during the spinup, although the magnitude of the increase is uncertain. Recorded iceberg keel plough marks from Petermann Glacier in Northern Greenland and Pine Island Glacier in West Antarctica during the Early Holocene show high frequency of ploughing, and individual plough marks as deep as 20 m (Wise et al., 2017; Jakobsson et al., 2018). We consider the setting of JI to be similar in regards to calving frequency and iceberg size. However, due to the narrower fjord the plough marks would be concentrated on a smaller area on the sill, thus creating a larger impact on the sill depth. We consider our assumption of sill erosion during the Mid and Late Holocene due to iceberg scouring likely.

The exact bathymetry of the fjord between the sill and the present day grounding line is highly uncertain due to difficulties in accessing the fjord. The errors of the bathymetry on the sill and in the trough beneath the present day ice sheet are smaller due to the better access with radar and gravimetry measurements, respectively. The error in the bathymetry of the fjord adds uncertainty to

the exact location of the bedrock bump, governing the Holocene minimum extent. However, the difference in depth before and after the bump is over 500 m, sufficient to exceed the error in the bathymetry (Morlighem et al., 2017). Thus, even if the exact location of the bump would shift slightly with changes in bathymetry, the dominant large scale feature remains. We interpret this bump as a tipping point, the passing of which determines the future evolution of the glacier, thus also constraining the minimum extent of the grounding line during the Holocene. It is noteworthy that this tipping point in the topography applies also to present day JI: once the grounding line retreats into the trough, it is not likely to readvance. In this case, a readvance to the present day position would require an intense period of cooling that would last for millenia, significantly longer than the duration of the LIA.

7. Conclusions

In this study, we use a high-resolution ice flow model to simulate the evolution of Jakobshavn Isbræ from the Mid-Holocene to the Little Ice Age. Our simulations show that Jakobshavn Isbræ remained close to the present day ice margin during the Mid-Holocene. The bedrock bump 60 km inland from the sill, where the present day grounding line is located, acts as a tipping point for Jakobshavn Isbræ grounding line migration. Our model shows that the glacier could not have retreated past this bump during the Holocene, as it would not have had time to readvance to the Little Ice Age moraine. The terrestrial margins show a minimum extent no more than 10 km inland from the present day ice margin.

In order to create the observed evolution of Jakobshavn Isbræ, both ocean cooling and atmospheric cooling are necessary. Jakobshavn Isbræ reacts rapidly to changes in melt rate: once the grounding line retreats behind the sill into the fjord, a significant ocean cooling is needed to halt the retreat and enable a readvance. At the same time, the readvance of the glacier requires an atmospheric cooling to increase the ice volume. However, the increase in ice volume takes millenia to influence the grounding line.

If the present day grounding line of Jakobshavn Isbræ were to retreat into the deep trough inland of its current position, the glacier would not be able to readvance without an intense period of cool climate persisting for millenia – significantly longer than the duration of the Little Ice Age.

Credit author statement

Karita Kajanto: Conceptualization, Software, Methodology, Visualization, Writing – original draft; Helene Seroussi: Software, Methodology, Writing – review and editing; Basile de Fleurian: Software, Visualization, Writing – review and editing; Kerim H. Nisancioglu: Conceptualization, Supervision, Writing – review and editing, Funding acquisition.

Declaration of competing interest

The authors declare that they have no known competing financial interests or personal relationships that could have appeared to influence the work reported in this paper.

Acknowledgements

We thank Benoit Lecavalier for sharing his model, and Mathieu Morlighem for valuable comments while setting up the ISSM model. We thank the Editor Colm O'Cofaigh and the reviewers Stewart Jamieson and Andreas Vieli for their thorough review and valuable comments. KK, BdF and KHN were supported by the European Research Council under the European Community's Seventh Framework Program (FP7/2007-2013)/ERC grant agreement 610055 as part of the ice2ice project. BdF is also funded the by SWItchDyn Norwegian Research Council (NRC) grant(287206). Funding for HS was provided by grants from NASA Cryospheric Science and Modeling, Analysis and Prediction (MAP) Programs. The simulations were performed on resources provided by UNINETT Sigma2 - the National Infrastructure for High Performance Computing and Data Storage in Norway (projects nn4659k and nn9635k).

Appendix A. Supplementary data

Supplementary data to this article can be found online at https://doi.org/10.1016/j.quascirev.2020.106492.

References

Åkesson, H., Nisancioglu, K.H., Nick, F.M., jun 2018. Impact of fjord geometry on grounding line stability. Front. Earth Sci. 6, 71. https://doi.org/10.3389/feart.2018.00071. ISSN 2296-6463. https://www.frontiersin.org/article/10.3389/feart.2018.00071/full.

An, L., Rignot, E., Elieff, S., Morlighem, M., Millan, R., Mouginot, J., Holland, D.M., Holland, D., Paden, J., apr 2017. Bed elevation of Jakobshavn Isbrae, West Greenland, from high-resolution airborne gravity and other data. Geophys. Res. Lett. 44 (8), 3728–3736. https://doi.org/10.1002/2017GL073245. ISSN 00948276.

Aschwanden, A., Fahnestock, M.A., Truffer, M., apr 2016. Complex Greenland outlet glacier flow captured. Nat. Commun. 7 (1), 10524. https://doi.org/10.1038/ncomms10524. ISSN 2041-1723.

Beaird, N., Straneo, F., Jenkins, W., apr 2017. Characteristics of meltwater export from Jakobshavn Isbræ and Ilulissat Icefjord. Ann. Glaciol. 58 (74), 107–117. https://doi.org/10.1017/aog.2017.19. ISSN 0260-3055.

Bondzio, J.H., Seroussi, H., Morlighem, M., Kleiner, T., Rückamp, M., Humbert, A., Larour, E.Y., mar 2016. Modelling calving front dynamics using a level-set method: application to Jakobshavn Isbræ, West Greenland. Cryosphere 10 (2), 497–510. https://doi.org/10.5194/tc-10-497-2016. ISSN 1994-0424.

Bondzio, J.H., Morlighem, M., Seroussi, H., Kleiner, T., Rückamp, M., Mouginot, J., Moon, T., Larour, E.Y., Humbert, A., jun 2017. The mechanisms behind Jakobshavn Isbrae's acceleration and mass loss: a 3-D thermomechanical model study. Geophys. Res. Lett. 44 (12), 6252–6260. https://doi.org/10.1002/2017GL073309. ISSN 00948276.

Briner, J., Stewart, H., Young, N., Philipps, W., Losee, S., dec 2010. Using proglacial-threshold lakes to constrain fluctuations of the Jakobshavn Isbræ ice margin, western Greenland, during the Holocene. Quat. Sci. Rev. 29 (27–28), 3861–3874. https://doi.org/10.1016/J.QUASCIREV.2010.09.005. ISSN 0277-3791.

Brondex, J., Gagliardini, O., Gillet-Chaulet, F., Durand, G., oct 2017. Sensitivity of grounding line dynamics to the choice of the friction law. J. Glaciol. 63 (241), 854–866. https://doi.org/10.1017/jog.2017.51. ISSN 0022-1430.

Budd, W.F., Keage, P.L., Blundy, N.A., jan 1979. Empirical studies of ice sliding. J. Glaciol. 23 (89), 157–170. https://doi.org/10.3189/S0022143000029804. ISSN 0022-1430.

Csatho, B., Schenk, T., Van Der Veen, C., Krabill, W.B., sep 2008. Intermittent thinning of Jakobshavn Isbræ, west Greenland, since the little ice age. J. Glaciol. 54 (184), 131–144. https://doi.org/10.3189/002214308784409035. ISSN 0022-1430.

Cuzzone, J.K., Schlegel, N.-J., Morlighem, M., Larour, E., Briner, J.P., Seroussi, H., Caron, L., mar 2019. The impact of model resolution on the simulated Holocene retreat of the southwestern Greenland ice sheet using the Ice Sheet System Model (ISSM). Cryosphere 13 (3), 879–893. https://doi.org/10.5194/tc-13-879-2019. ISSN 1994-0424.

Durand, G., Gagliardini, O., de Fleurian, B., Zwinger, T., Le Meur, E., aug 2009. Marine ice sheet dynamics: hysteresis and neutral equilibrium. J. Geophys. Res. 114 (F3), F03009. https://doi.org/10.1029/2008JF001170. ISSN 0148-0227.

Enderlin, E.M., Howat, I.M., Jeong, S., Noh, M.-J., van Angelen, J.H., van den Broeke, M.R., feb 2014. An improved mass budget for the Greenland ice sheet. Geophys. Res. Lett. 41 (3), 866–872. https://doi.org/10.1002/2013GL059010. ISSN 00948276.

Fleming, K., Lambeck, K., may 2004. Constraints on the Greenland ice sheet since the last glacial maximum from sea-level observations and glacial-rebound models. Quat. Sci. Rev. 23 (9–10), 1053–1077. https://doi.org/10.1016/J.QUASCIREV.2003.11.001. ISSN 0277-3791.

Funder, S., Kjeldsen, K.K., Kjær, K.H., O Cofaigh, C., 2011. The Greenland Ice Sheet during the Past 300,000 Years: A Review. https://doi.org/10.1016/B978-0-444-53447-7.00050-7.

Glen, J., mar 1955. The creep of polycrystalline ice. Proc. Roy. Soc. Lond. Math. Phys. Sci. 228 (1175), 519–538. https://doi.org/10.1098/rspa.1955.0066. ISSN 2053-9169.

Greve, R., Herzfeld, U.C., jul 2013. Resolution of ice streams and outlet glaciers in large-scale simulations of the Greenland ice sheet. Ann. Glaciol. 54 (63), 209–220. https://doi.org/10.3189/2013AoG63A085. ISSN 0260-3055.

Gudmundsson, G.H., Krug, J., Durand, G., Favier, L., Gagliardini, O., dec 2012. The stability of grounding lines on retrograde slopes. Cryosphere 6 (6), 1497–1505. https://doi.org/10.5194/tc-6-1497-2012. ISSN 1994-0424.

Helsen, M.M., van de Wal, R.S.W., van den Broeke, M.R., van de Berg, W.J., Oerlemans, J., mar 2012. Coupling of climate models and ice sheet models by surface mass balance gradients: application to the Greenland Ice Sheet. Cryosphere 6 (2), 255–272. https://doi.org/10.5194/tc-6-255-2012. ISSN 1994-0424.

Hogan, K., Dowdeswell, J., Ó Cofaigh, C., may 2012. Glacimarine sedimentary processes and depositional environments in an embayment fed by West Greenland ice streams. Mar. Geol. 311–314, 1–16. https://doi.org/10.1016/J.MARGEO.2012.04.006. ISSN 0025-3227.

Hogan, K.A., Jennings, A.E., Dowdeswell, J.A., Hiemstra, J.F., sep 2016. Deglaciation of a major palaeo-ice stream in Disko trough, west Greenland. Quat. Sci. Rev. 147, 5–26. https://doi.org/10.1016/J.QUASCIREV.2016.01.018. ISSN 0277-3791.

Humlum, O., 1987. Glacier behaviour and the influence of upper-air conditions during the little ice age in Disko, central west Greenland. Geografisk Tidsskrift - Danish J. Geogr. 87 (1), 1–12.

Huybrechts, P., jan 2002. Sea-level changes at the LGM from ice-dynamic reconstructions of the Greenland and Antarctic ice sheets during the glacial cycles. Quat. Sci. Rev. 21 (1–3), 203–231. https://doi.org/10.1016/S0277-3791(01)00082-8. ISSN 0277-3791.

Jakobsson, M., Hogan, K.A., Mayer, L.A., Mix, A., Jennings, A., Stoner, J., Eriksson, B., Jerram, K., Mohammad, R., Pearce, C., Reilly, B., Stranne, C., dec 2018. The Holocene retreat dynamics and stability of Petermann Glacier in northwest Greenland. Nat. Commun. 9 (1), 2104. https://doi.org/10.1038/s41467-018-04573-2. ISSN 2041-1723.

Jamieson, S.S.R., Vieli, A., Livingstone, S.J., Cofaigh, C.Ó., Stokes, C., Hillenbrand, C.-D., Dowdeswell, J.A., nov 2012. Ice-stream stability on a reverse bed slope. Nat. Geosci. 5 (11), 799–802. https://doi.org/10.1038/ngeo1600. ISSN 1752-0894.

Jamieson, S.S.R., Vieli, A., Cofaigh, C.Ó., Stokes, C.R., Livingstone, S.J., Hillenbrand, C.-D., feb 2014. Understanding controls on rapid ice-stream retreat during the last deglaciation of Marguerite Bay, Antarctica, using a numerical model. J. Geophys. Res.: Earth Surface 119 (2), 247–263. https://doi.org/10.1002/2013JF002934. ISSN 21699003.

Joughin, I., Howat, I.M., Fahnestock, M., Smith, B., Krabill, W., Alley, R.B., Stern, H., Truffer, M., oct 2008. Continued evolution of Jakobshavn Isbrae following its rapid speedup. J. Geophys. Res. 113 (F4), F04006. https://doi.org/10.1029/2008JF001023. ISSN 0148-0227.

Joughin, I., Smith, B.E., Howat, I.M., Floricioiu, D., Alley, R.B., Truffer, M., Fahnestock, M., jun 2012. Seasonal to decadal scale variations in the surface velocity of Jakobshavn Isbrae, Greenland: observation and model-based analysis. n/a–n/a J. Geophys. Res.: Earth Surface 117 (F2). https://doi.org/10.1029/2011JF002110. ISSN 01480227.

Khazendar, A., Fenty, I.G., Carroll, D., Gardner, A., Lee, C.M., Fukumori, I., Wang, O., Zhang, H., Seroussi, H., Moller, D., Noël, B.P.Y., van den Broeke, M.R., Dinardo, S., Willis, J., apr 2019. Interruption of two decades of Jakobshavn Isbrae acceleration and thinning as regional ocean cools. Nat. Geosci. 12 (4), 277–283. https://doi.org/10.1038/s41561-019-0329-3. ISSN 1752-0894.

Krawczyk, D.W., Witkowski, A., Moros, M., Lloyd, J.M., Høyer, J.L., Miettinen, A., Kuijpers, A., jan 2017. Quantitative reconstruction of Holocene sea ice and sea surface temperature off West Greenland from the first regional diatom data set. Paleoceanography 32 (1), 18–40. https://doi.org/10.1002/2016PA003003. ISSN 08838305.

Larour, E., Seroussi, H., Morlighem, M., Rignot, E., mar 2012. Continental scale, high order, high spatial resolution, ice sheet modeling using the Ice Sheet System Model (ISSM). n/a–n/a J. Geophys. Res.: Earth Surface 117 (F1). https://doi.org/10.1029/2011JF002140. ISSN 01480227.

Lecavalier, B.S., Milne, G.A., Simpson, M.J.R., Wake, L., Huybrechts, P., Tarasov, L., Kjeldsen, K.K., Funder, S., Long, A.J., Woodroffe, S., Dyke, A.S., Larsen, N.K., oct 2014. A model of Greenland ice sheet deglaciation constrained by observations of relative sea level and ice extent. Quat. Sci. Rev. 102, 54–84. https://doi.org/10.1016/J.QUASCIREV.2014.07.018. ISSN 0277-3791.

Lesnek, A.J., Briner, J.P., jan 2018. Response of a land-terminating sector of the western Greenland Ice Sheet to early Holocene climate change: evidence from 10Be dating in the Søndre Isortoq region. Quat. Sci. Rev. 180, 145–156. https://doi.org/10.1016/J.QUASCIREV.2017.11.028. ISSN 0277-3791.

Lloyd, J., Park, L., Kuijpers, A., Moros, M., aug 2005. Early Holocene palaeoceanography and deglacial chronology of Disko Bugt, west Greenland. Quat. Sci. Rev. 24 (14–15), 1741–1755. https://doi.org/10.1016/J.QUASCIREV.2004.07.024. ISSN 0277-3791.

Lloyd, J., Moros, M., Perner, K., Telford, R.J., Kuijpers, A., Jansen, E., McCarthy, D., sep 2011. A 100 yr record of ocean temperature control on the stability of Jakobshavn Isbrae, West Greenland. Geology 39 (9), 867–870. https://doi.org/10.1130/G32076.1. ISSN 0091-7613.

Long, A., Roberts, D., Dawson, S., may 2006. Early Holocene history of the West Greenland ice sheet and the GH-8.2 event. Quat. Sci. Rev. 25 (9–10), 904–922. https://doi.org/10.1016/J.QUASCIREV.2005.07.002. ISSN 0277-3791.

MacAyeal, D.R., apr 1989. Large-scale ice flow over a viscous basal sediment: theory and application to ice stream B, Antarctica. J. Geophys. Res.: Solid Earth 94 (B4), 4071–4087. https://doi.org/10.1029/JB094iB04p04071. ISSN 01480227.

Morland, L.W., 1987. Unconfined Ice-Shelf Flow. Springer, Dordrecht, pp. 99–116. https://doi.org/10.1007/978-94-009-3745-16.

Morlighem, M., Bondzio, J., Seroussi, H., Rignot, E., Larour, E., Humbert, A., Rebuffi, S., mar 2016. Modeling of Store Gletscher's calving dynamics, West Greenland, in response to ocean thermal forcing. Geophys. Res. Lett. 43 (6), 2659–2666. https://doi.org/10.1002/2016GL067695. ISSN 0094-8276.

Morlighem, M., Williams, C.N., Rignot, E., An, L., Arndt, J.E., Bamber, J.L., Catania, G., Chauché, N., Dowdeswell, J.A., Dorschel, B., Fenty, I., Hogan, K., Howat, I., Hubbard, A., Jakobsson, M., Jordan, T.M., Kjeldsen, K.K., Millan, R., Mayer, L., Mouginot, J., Noël, B.P.Y., O'Cofaigh, C., Palmer, S., Rysgaard, S., Seroussi, H., Siegert, M.J., Slabon, P., Straneo, F., van den Broeke, M.R., Weinrebe, W., Wood, M., Zinglersen, K.B., nov 2017. BedMachine v3: complete bed topography and ocean bathymetry mapping of Greenland from multibeam echo sounding combined with mass conservation. Geophys. Res. Lett. 44 (21), 11,051–11,061. https://doi.org/10.1002/2017GL074954. ISSN 00948276.

Moros, M., Lloyd, J.M., Perner, K., Krawczyk, D., Blanz, T., de Vernal, A., Ouellet-Bernier, M.-M., Kuijpers, A., Jennings, A.E., Witkowski, A., Schneider, R., Jansen, E., jan 2016. Surface and sub-surface multi-proxy reconstruction of middle to late Holocene palaeoceanographic changes in Disko Bugt, West Greenland. Quat. Sci. Rev. 132, 146–160. https://doi.org/10.1016/J.QUASCIREV.2015.11.017. ISSN 0277-3791.

Muresan, I.S., Khan, S.A., Aschwanden, A., Khroulev, C., Dam, T.V., Bamber, J., Van Den Broeke, M.R., Wouters, B., Munneke, P.K., Kjaer, K.H., 2016. Modelled glacier dynamics over the last quarter of a century at Jakobshavn Isbrae. Cryosphere 10, 597–611. https://doi.org/10.5194/tc-10-597-2016.

Nick, F.M., Vieli, A., Andersen, M.L., Joughin, I., Payne, A., Edwards, T.L., Pattyn, F., Van De Wal, R.S., 2013. Future sea-level rise from Greenland's main outlet glaciers in a warming climate. Nature 497 (7448), 235–238. https://doi.org/10.1038/nature12068. ISSN 00280836.

Nielsen, L.T., Aðalgeirsdóttir, G., Gkinis, V., Nuterman, R., Hvidberg, C.S., jun 2018. The effect of a Holocene climatic optimum on the evolution of the Greenland ice sheet during the last 10 kyr. J. Glaciol. 64 (245), 477–488. https://doi.org/10.1017/jog.2018.40. ISSN 0022-1430.

Nye, J., apr 1957. The distribution of stress and velocity in glaciers and ice-sheets. Proc. Roy. Soc. Lond. Math. Phys. Sci. 239 (1216), 113–133. https://doi.org/10.1098/rspa.1957.0026. ISSN 2053-9169.

O Cofaigh, C., Dowdeswell, J.A., Jennings, A.E., Hogan, K.A., Kilfeather, A., Hiemstra, J.F., Noormets, R., Evans, J., McCarthy, D.J., Andrews, J.T., Lloyd, J.M., Moros, M., feb 2013. An extensive and dynamic ice sheet on the West Greenland shelf during the last glacial cycle. Geology 41 (2), 219–222. https://doi.org/10.1130/G33759.1. ISSN 0091-7613.

Perner, K., Moros, M., Snowball, I., Lloyd, J.M., Kujipers, A., Richter, T., jul 2013. Establishment of modern circulation pattern at c . 6000 cal a BP in Disko Bugt, central West Greenland: opening of the Vaigat Strait. J. Quat. Sci. 28 (5), 480–489. https://doi.org/10.1002/jqs.2638. ISSN 02678179.

Plach, A., Nisancioglu, K.H., Le clec'h, S., Born, A., Langebroek, P.M., Guo, C., Imhof, M., Stocker, T.F., oct 2018. Eemian Greenland SMB strongly sensitive to model choice. Clim. Past 14 (10), 1463–1485. https://doi.org/10.5194/cp-14-1463-2018. ISSN 1814-9332.

Rignot, E., Mouginot, J., jun 2012. Ice flow in Greenland for the international polar year 2008-2009. n/a–n/a Geophys. Res. Lett. 39 (11). https://doi.org/10.1029/2012GL051634. ISSN 00948276.

Schoof, C., jul 2007. Ice sheet grounding line dynamics: steady states, stability, and hysteresis. J. Geophys. Res. 112 (F3), F03S28. https://doi.org/10.1029/2006JF000664. ISSN 0148-0227.

Schweinsberg, A.D., Briner, J.P., Miller, G.H., Bennike, O., Thomas, E.K., mar 2017. Local glaciation in West Greenland linked to north Atlantic ocean circulation during the Holocene. Geology 45 (3), 195–198. https://doi.org/10.1130/G38114.1. ISSN 0091-7613.

Seroussi, H., Morlighem, M., Rignot, E., Khazendar, A., Larour, E., Mouginot, J., jul 2013. Dependence of century-scale projections of the Greenland ice sheet on its thermal regime. J. Glaciol. 59 (218), 1024–1034. https://doi.org/10.3189/2013JoG13J054. ISSN 0022-1430.

Seroussi, H., Morlighem, M., Larour, E., Rignot, E., Khazendar, A., nov 2014. Hydrostatic grounding line parameterization in ice sheet models. Cryosphere 8 (6), 2075–2087. https://doi.org/10.5194/tc-8-2075-2014. ISSN 1994-0424.

Simpson, M.J., Milne, G.A., Huybrechts, P., Long, A.J., aug 2009. Calibrating a glaciological model of the Greenland ice sheet from the Last Glacial Maximum to present-day using field observations of relative sea level and ice extent. Quat. Sci. Rev. 28 (17–18), 1631–1657. https://doi.org/10.1016/J.QUASCIREV.2009.03.004. ISSN 0277-3791.

Steiger, N., Nisancioglu, K.H., Åkesson, H., de Fleurian, B., Nick, F.M., jul 2018. Simulated retreat of Jakobshavn Isbræ since the little ice age controlled by geometry. Cryosphere 12 (7), 2249–2266. https://doi.org/10.5194/tc-12-2249-2018. ISSN 1994-0424.

Straneo, F., Heimbach, P., Sergienko, O., Hamilton, G., Catania, G., Griffies, S., Hallberg, R., Jenkins, A., Joughin, I., Motyka, R., Pfeffer, W.T., Price, S.F., Rignot, E., Scambos, T., Truffer, M., Vieli, A., 2013. Challenges to understanding the dynamic response of Greenland's marine terminating glaciers to oc eanic and atmospheric forcing. Bull. Am. Meteorol. Soc. 94 (8), 1131–1144. https://doi.org/10.1175/BAMS-D-12-00100.1. ISSN 00030007.

Streuff, K., Ó Cofaigh, C., Hogan, K., Jennings, A., Lloyd, J.M., Noormets, R., Nielsen, T., Kuijpers, A., Dowdeswell, J.A., Weinrebe, W., aug 2017. Seafloor geomorphology and glacimarine sedimentation associated with fast-flowing ice sheet outlet glaciers in Disko Bay, West Greenland. Quat. Sci. Rev. 169, 206–230. https://doi.org/10.1016/j.quascirev.2017.05.021. ISSN 02773791.

Tabone, I., Robinson, A., Alvarez-Solas, J., Montoya, M., mar 2019. Impact of millennial-scale oceanic variability on the Greenland ice-sheet evolution throughout the last glacial period. Clim. Past 15 (2), 593–609. https://doi.org/10.5194/cp-15-593-2019. ISSN 1814-9332.

Tarasov, L., Peltier, R., jul 2002. Greenland glacial history and local geodynamic consequences. Geophys. J. Int. 150 (1), 198–229. https://doi.org/10.1046/j.1365-246X.2002.01702.x. ISSN 0956540X.

Van Der Veen, C., Plummer, J.C., Stearns, L., sep 2011. Controls on the recent speed-up of Jakobshavn Isbræ, west Greenland. J. Glaciol. 57 (204), 770–782. https://doi.org/10.3189/002214311797409776. ISSN 0022-1430.

Vieli, A., Nick, F.M., sep 2011. Understanding and modelling rapid dynamic changes of tidewater outlet glaciers: issues and implications. Surv. Geophys. 32 (4–5), 437–458. https://doi.org/10.1007/s10712-011-9132-4. ISSN 0169-3298.

Vinther, B.M., Buchardt, S.L., Clausen, H.B., Dahl-Jensen, D., Johnsen, S.J., Fisher, D.A., Koerner, R.M., Raynaud, D., Lipenkov, V., Andersen, K.K., Blunier, T., Rasmussen, S.O., Steffensen, J.P., Svensson, A.M., sep 2009. Holocene thinning of the Greenland ice sheet. Nature 461 (7262), 385–388. https://doi.org/10.1038/nature08355. ISSN 0028-0836.

Wangner, D.J., Jennings, A.E., Vermassen, F., Dyke, L.M., Hogan, K.A., Schmidt, S., Kjær, K.H., Knudsen, M.F., Andresen, C.S., nov 2018. A 2000-year record of ocean influence on Jakobshavn Isbræ calving activity, based on marine sediment cores. Holocene 28 (11), 1731–1744. https://doi.org/10.1177/0959683618788701. ISSN 0959-6836. http://journals.sagepub.com/doi/10.1177/0959683618788701.

Weidick, A., Bennike, O., 2007. Quaternary Glaciation History and Glaciology of Jakobshavn Isbrae and the Disko Bugt Region, West Greenland : a Review. Geological Survey of Denmark and Greenland. ISBN 9788778712073.

Weidick, A., Oerter, H., Reeh, N., Thomsen, H.H., Thorning, L., aug 1990. The recession of the inland ice margin during the Holocene climatic optimum in the Jakobshavn Isfjord area of west Greenland. Palaeogeogr. Palaeoclimatol. Palaeoecol. 82 (3–4), 389–399. https://doi.org/10.1016/S0031-0182(12)80010-1. ISSN 0031-0182.

Wilson, N., Straneo, F., Heimbach, P., dec 2017. Satellite-derived submarine melt rates and mass balance (2011â€“2015) for Greenland's largest remaining ice tongues. Cryosphere 11 (6), 2773–2782. https://doi.org/10.5194/tc-11-2773-2017. ISSN 1994-0424.

Wise, M.G., Dowdeswell, J.A., Jakobsson, M., Larter, R.D., oct 2017. Evidence of marine ice-cliff instability in Pine Island Bay from iceberg-keel plough marks. Nature 550 (7677), 506–510. https://doi.org/10.1038/nature24458. ISSN 14764687.

Young, N.E., Briner, J.P., apr 2015. Holocene evolution of the western Greenland Ice Sheet: assessing geophysical ice-sheet models with geological reconstructions of ice-margin change. Quat. Sci. Rev. 114 (1–17) https://doi.org/10.1016/J.QUASCIREV.2015.01.018. ISSN 0277-3791.